T-tubule disorganization and defective excitation-contraction coupling in muscle fibers lacking myotubularin lipid phosphatase

Lama Al-Qusairi[a], Norbert Weiss[b], Anne Toussaint[a], Céline Berbey[b], Nadia Messaddeq[c], Christine Kretz[a], Despina Sanoudou[d,1], Alan H. Beggs[d], Bruno Allard[b], Jean-Louis Mandel[a], Jocelyn Laporte[a], Vincent Jacquemond[b], and Anna Buj-Bello[a,2,3]

[a]Department of Neurobiology and Genetics, and [c]Imaging Center—Electron Microscopy, Institut de Génétique et de Biologie Moléculaire et Cellulaire, Institut National de la Santé et de la Recherche Médicale U964, Centre National de la Recherche Scientifique, Unite Mixte de Recherche 7104, Université Louis Pasteur, Collège de France, 67404 Illkirch, France; [b]Unite Mixte de Recherche 5123, Université Lyon 1, 69622 Villeurbanne, France; and [d]Genetics Division and Program in Genomics, The Manton Center for Orphan Disease Research, Children's Hospital Boston, Harvard Medical School, Boston, MA 02115

Edited by Louis M. Kunkel, Harvard Medical School, Boston, MA, and approved September 18, 2009 (received for review January 22, 2009)

Skeletal muscle contraction is triggered by the excitation-contraction (E-C) coupling machinery residing at the triad, a membrane structure formed by the juxtaposition of T-tubules and sarcoplasmic reticulum (SR) cisternae. The formation and maintenance of this structure is key for muscle function but is not well characterized. We have investigated the mechanisms leading to X-linked myotubular myopathy (XLMTM), a severe congenital disorder due to loss of function mutations in the *MTM1* gene, encoding myotubularin, a phosphoinositide phosphatase thought to have a role in plasma membrane homeostasis and endocytosis. Using a mouse model of the disease, we report that *Mtm1*-deficient muscle fibers have a decreased number of triads and abnormal longitudinally oriented T-tubules. In addition, SR Ca^{2+} release elicited by voltage-clamp depolarizations is strongly depressed in myotubularin-deficient muscle fibers, with myoplasmic Ca^{2+} removal and SR Ca^{2+} content essentially unaffected. At the molecular level, *Mtm1*-deficient myofibers exhibit a 3-fold reduction in type 1 ryanodine receptor (RyR1) protein level. These data reveal a critical role of myotubularin in the proper organization and function of the E-C coupling machinery and strongly suggest that defective RyR1-mediated SR Ca^{2+} release is responsible for the failure of muscle function in myotubular myopathy.

myotubular myopathy | triad

X-linked myotubular (centronuclear) myopathy (XLMTM; OMIM 310400) is a severe congenital disorder characterized by generalized muscle weakness and hypotonia often leading to poor vital prognosis during early infancy. XLMTM belongs to a group of muscular disorders named centronuclear myopathies (CNM) that share a common pathological feature in skeletal muscle, the presence of hypotrophic myofibers with internal nuclei (1–3). More than 200 loss-of-function mutations in the *MTM1* gene, affecting all domains of the *MTM1* gene product, myotubularin, have been identified in patients with myotubular myopathy (4–6). Myotubularin is a ubiquitously expressed phosphoinositide (PI) 3-phosphatase that acts on both phosphatidylinositol 3-phosphate [PI(3)P] and 3,5-bisphosphate [$PI(3,5)P_2$] in vitro and in vivo (7–10). These signaling lipids play important functions in the endocytic pathway by regulating the temporal recruitment of proteins required for endosome maturation, protein sorting, and lysosomal degradation (11–13). Although the enzymatic and cellular functions of myotubularin have been investigated in cell lines, the specific role(s) of this protein in muscle cells remains unknown.

In autosomal cases of CNM, mutations have been found to date in the *DNM2* gene encoding the large GTPase dynamin 2 (14) and in the *BIN1* gene encoding amphiphysin 2 (15), two proteins known to regulate membrane remodeling and trafficking and implicated in endocytosis. In particular, amphiphysin 2 is localized at transverse (T)-tubules in muscle, and a muscle-specific isoform of amphiphysin 2 has membrane tubulation properties (16, 17). Recent expression studies in mouse have shown that myotubularin is partly associated with the triads of muscle fibers (18).

In skeletal muscle, triads are membrane structures composed of a T-tubule, which results from the onward invagination of the plasma membrane, and two terminal cisternae of sarcoplasmic reticulum (SR), where excitation-contraction (E-C) coupling occurs (19). In mammalian muscles, E-C coupling relies on a tight control of SR Ca^{2+} release via the type 1 ryanodine receptor (RyR1) by the voltage-sensing dihydropyridine receptor (DHPR). RyR1 is located at the junctional terminal cisternae of the SR and interacts with the DHPR complex. Depolarization of the T-tubule membrane causes a conformational change in the $Ca_v1.1$ subunit ($DHPR\alpha_1$) that directly activates the RyR1. This allows rapid mobilization of the SR Ca^{2+} store resulting in a rise in myoplasmic [Ca^{2+}] that triggers contraction. Conversely, muscle relaxation occurs through Ca^{2+} re-uptake into the SR by ATP-dependent sarco(endo)plasmic reticulum Ca^{2+} pumps (SERCAs) (19).

Studies of rodent models deficient for *Mtm1* have revealed that skeletal muscle is indeed the primary tissue involved in the pathogenesis of XLMTM and that myotubularin is essential for muscle growth and proper distribution of organelles in myofibers. Myotubularin knockout (KO) mice develop a CNM, starting at around 3–4 weeks of postnatal age, with progressive muscle weakness that severely reduces life expectancy to about 6–12 weeks (20). The molecular mechanisms responsible for these structural abnormalities and force deficit are currently unknown.

In this study, we investigated the mechanisms responsible for the loss of muscle function in XLMTM. We characterized the morphological and functional properties of the E-C coupling machinery in muscle fibers lacking myotubularin PIs phospha-

Author contributions: N.W., A.H.B., B.A., J.-L.M., J.L., V.J., and A.B.-B. designed research; L.A.-Q., N.W., A.T., C.B., N.M., C.K., D.S., and B.A. performed research; L.A.-Q., N.W., A.T., C.B., N.M., D.S., A.H.B., B.A., J.L., V.J., and A.B.-B. analyzed data; and J.-L.M., J.L., V.J., and A.B.-B. wrote the paper.

The authors declare no conflict of interest.

This article is a PNAS Direct Submission.

[1]Present address: Molecular Biology Division, Biomedical Research Foundation, Academy of Athens, Athens 115 27, Greece, and Department of Pharmacology, Medical School, National and Kapodistrian University of Athens, Greece.

[2]Present address: Généthon, 91000 Evry, France.

[3]To whom correspondence may be addressed. E-mail: abujbello@genethon.fr or mtm@igbmc.fr.

This article contains supporting information online at www.pnas.org/cgi/content/full/0900705106/DCSupplemental.

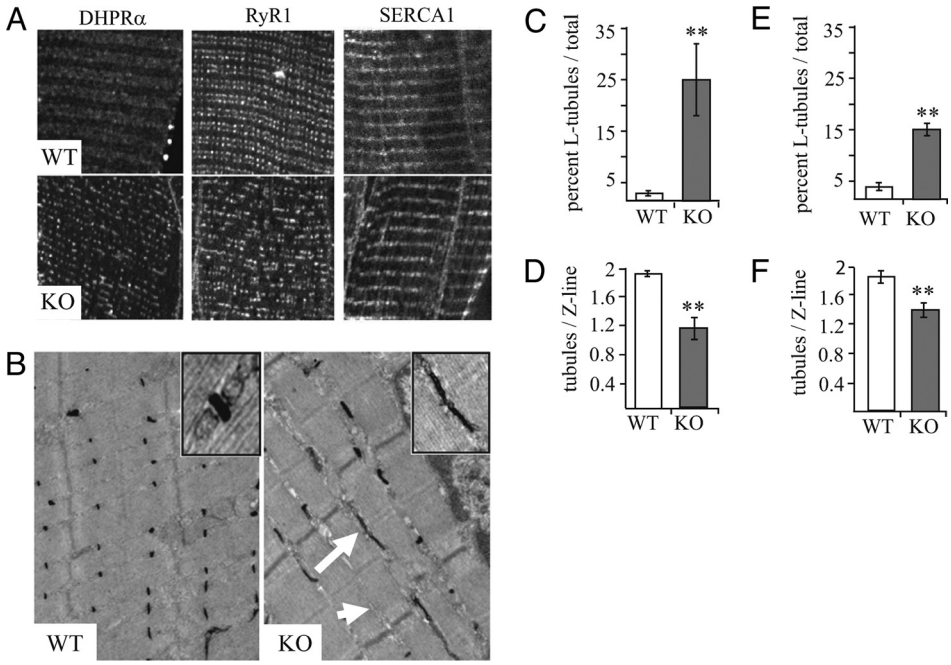

Fig. 1. Triad disorganization in myotubularin-deficient muscle. (*A*) Distribution of T-tubules and SR in semithin sections of skeletal muscle from 5-week-old WT and *Mtm1* KO mice by immunolabeling of DHPRα, RYR1, and SERCA1. (*B*) Electron micrographs of WT and KO muscle labeled with the potassium ferrocyanide [$K_3Fe(CN)_6$] procedure. Electron dense material is located within the lumen of T-tubules (see high magnification in WT and KO micrographs). Upper arrow shows the presence of a L-tubule in mutant muscle. Bottom arrow shows a missing T-tubule/triad. (*C*) Percentage of L-tubules (2 ± 0.4) in WT and (26 ± 4.8) in KO muscle fibers of mice at 5 weeks of age ($P < 0.001$). (*D*) Percentage of tubules per Z-line in myofibers of 5-week-old mice ($P < 0.001$). (*E*) Percentage of L-tubules in muscle fibers of mice at 2 weeks of age (3.6 ± 0.3 for WT and 15 ± 1.1 KO, $P < 0.001$). (*F*) Percentage of tubules per Z-line in myofibers of 2-week-old mice ($P < 0.001$). Data were obtained from $n = 16$ TA muscle fibers of four WT and four KO mice at both 5 and 2 weeks of age.

tase and uncovered structural anomalies of T-tubules and defects in SR calcium release, suggesting that E-C uncoupling is responsible for the muscle weakness in XLMTM.

Results

Abnormal Distribution of Triads in Myotubularin-Deficient Myofibers. In this study, we used a constitutive *Mtm1* KO line in the 129PAS background, because mutant mice develop a clinically more homogenous and severe CNM than previously characterized in C57/Bl6 KO mice (20). These mutant animals develop a progressive growth impairment, with a 10–15% reduction of weight during the first 4 postnatal weeks as compared to wild-type (WT) littermates, reaching about 30% from 5 weeks of age (see Fig. S1). *Mtm1*-deficient mice manifest a progressive muscle weakness, starting clinically at around 3–4 weeks, and most of them are dead by the age of 7 weeks (mean = 38.6 ± 7.1 days, range = 28–54, $n = 11$). In 5-week-old mutant mice, the weight of the tibialis anterior (TA) muscle is lower by 50% compared to controls, the corresponding mean cross-sectional area of myofibers is significantly smaller (554 μm^2 in KO versus 1,260 μm^2 in WT), and the percentage of internalized nuclei is 10 ± 3.9 compared to 1.6 ± 0.3 in WT mice (see Fig. S1). Fig. S1 also shows that the distribution of oxidative staining, which reflects the position of mitochondria and ER, is abnormal in mutant TA myofibers and adopts a "necklace" aspect with accumulation of staining in the subsarcolemmal region, as observed in XLMTM patients (21) and a "core-like" aspect, with reduction of staining in the center of fibers, as seen in myopathies due to *RYR1* mutations (22). Central aggregation of NADH-TR staining (mitochondria), a hallmark of XLMTM pathology, is also observed.

Since myotubularin is partly associated with triads in skeletal muscle (18) and transcriptome studies from XLMTM murine muscle revealed disturbances in expression of some genes implicated in Ca^{2+} homeostasis including *Cacng1* (2.2-fold up), *Homer1* (2.4-fold down), *Camk2D* (3.2-fold up), *Chrna1* (6.7-fold up), *Rrad* (61-fold up), and *Sln* (72-fold up), we investigated the E-C coupling machinery in this animal model. We analyzed at 5 weeks the distribution of triads by immunolabeling markers of T-tubules (DHPR) and terminal cisternae of SR (RyR1). The longitudinal SR membrane was monitored by SERCA1 ATPase labeling. We observed abnormal localization of some of these markers compared to WT muscles where they aligned as a typical striated pattern reflecting the organization of myofibrils (Fig. 1*A*). In *Mtm1* KO muscles, DHPRα and RyR1 striations were disorganized with absence of labeling in some regions and occasional divergence from the transversal orientation, while SERCA1 distribution appeared mostly normal. This suggests a disorganization of both T-tubules and terminal SR cisternae.

We further analyzed the morphology of triads at the ultrastructural level by electron microscopy using potassium ferrocyanide as a selective staining procedure for T-tubules. In 5-week-old mutant TA myofibers, we found a significant proportion of tubules with longitudinal orientation that are aligned to the direction of myofibrils (Fig. 1*B*). This distribution is very rare in normal muscle at this age (less than 6% of total tubules) and was found in 11 out of 16 mutant fibers. Longitudinal (L)-tubules represents 25% of total tubules in analyzed KO myofibers ($n = 16$ fibers from both four WT and four *Mtm1* KO mice) (Fig. 1*C*). We also measured the number of tubules (T- and L-tubules) per Z-line, which reflects the distribution of triads along myofibrils, and corresponds to about two in normal mature muscle cells. Fig. 1*D* shows that there is a 40% decrease in the number of triads in mutant fibers at this age (mean 1.09 ± 0.1 in KO versus 1.86 ± 0.03 in WT, $P < 0.001$).

To know whether these T-tubule abnormalities are already present at early stages of disease progression, we investigated 2-week-old KO mice. At this age, weakness could not be observed in hind limbs, but muscle weight was already decreased,

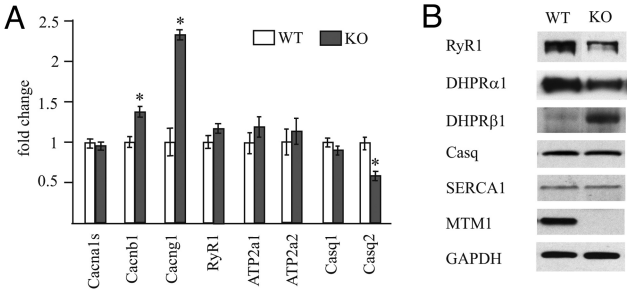

Fig. 2. Dysregulation of genes involved in calcium homeostasis in mutant mice. (*A*) Fold change of DHPRα_1, β_1, and γ_1 subunits (*Cacna1s*, *Cacnb1*, and *Cacng1*), type 1 ryanodine receptor (*RyR1*), type 1 and 2 SERCA pumps (*Atp2a1*, *Atp2a2*), and calsequestrin 1 and 2 (*Casq1*, *Casq2*) mRNA levels in KO versus WT TA muscle in 5-week-old mice ($n = 3$ samples for both WT and KO, $P = 0.01$ for both *Cacnb1* and *Casq2*, and $P = 0.03$ for Cacng1; each sample was analyzed as triplicates). (*B*) Immunoblots show that the protein level of RYR1 and DHPRα_1 are decreased in TA mutant muscle at 5 weeks, whereas DHPRβ_1 level is higher (for DHPRα_1, $n = 4$, biological samples were analyzed from both WT and KO mice, $P = 0.05$, and $n = 7$, TA samples of each genotype were used to quantify the level of the other proteins, $P = 0.004$ for RYR1 and $P < 0.001$ for DHPRβ_1).

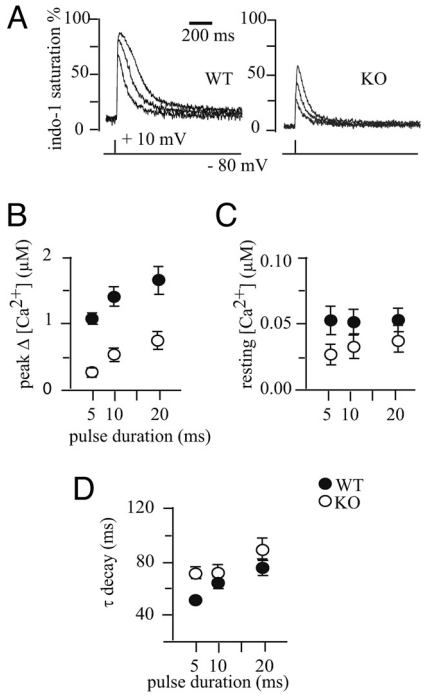

Fig. 3. E-C coupling defects in muscle fibers from *Mtm1* KO mice. (*A*) Indo-1 calcium transients elicited by voltage-clamp depolarizations of 5, 10, and 20 ms duration from −80 mV to +10 mV in a WT (left) and KO (right) muscle fiber. (*B–D*) Graphs show mean values for peak $\Delta[Ca^{2+}]$, resting $[Ca^{2+}]$, and time constant of $[Ca^{2+}]$ decay after the end of the pulse for indo-1 transients measured under the same conditions as in panel *A* ($n = 14$ and 14, fibers from two WT and two KO mice, respectively).

mitochondria appeared partly mislocalized, and the percentage of internal nuclei was slightly increased in KO muscle (see Fig. S2). Indeed, L-tubules were also more frequent in mutants at this early stage of the disease from about 4% in WT to a mean value of 15% in KO fibers (Fig. 1*E*). In addition, we found that the number of tubules per Z-line was already lower by about 25% in *Mtm1*-deficient muscle fibers at this age (1.37 ± 0.07 and 1.81 ± 0.06 in KO and WT fibers, respectively, $P < 0.001$) (Fig. 1*F*).

Altogether, these results indicate that myotubularin is important for the proper organization of the T-tubules and triads in skeletal muscle and that triad disorganization is an early event in the pathogenesis of the disease in these mice that progresses over time.

Absence of Myotubularin Leads To Dysregulation of Genes Involved in Calcium Homeostasis. We also examined the expression level of key regulators of the E-C coupling process in TA muscle. By using quantitative RT-PCR, we measured the mRNA level of the α_1, β_1, and γ_1 subunits of the voltage-sensing DHPR (*Cacna1s*, *Cacnb1*, and *Cacng1*), the SR Ca^{2+} release channel type 1 ryanodine receptor (*RyR1*), type 1 and 2 SERCA pumps (*Atp2a1*, *Atp2a2*), and calsequestrin 1 and 2 (*Casq1*, *Casq2*), which encode the major Ca^{2+}-buffering proteins in the lumen of striated muscle SR (23). In 5-week-old-mice, we found that *Cacnb1* and *Cacng1* mRNAs were significantly increased by 1.3- and 3-fold, respectively, whereas transcript level of *Casq2* was decreased by about 30% (Fig. 2*A*). The expression of *Cacng1* was already augmented in mutant muscle at 2 weeks of age (*SI Methods* and Fig. S3).

Given these data, we quantified DHPRα_1, DHPRβ_1, RyR1, SERCA1, and calsequestrin protein level in TA muscle of *Mtm1* null mice during disease evolution. We found that the ryanodine receptor was strikingly reduced by 3-fold in microsomal preparations of KO muscles at 5 weeks of age and DHPRα_1 was decreased by about 30%, whereas DHPRβ_1 level was about 6-fold higher (Fig. 2*B* and Fig. S3). Discrepancies between the mRNA and protein levels of *Ryr1* and *Cacna1s* may result from decreased protein stability, possibly due to an alteration in RYR1-DHPR interaction. All these proteins were also analyzed in muscle from 2-week-old mice, when weakness was not visible, and we found no significant differences between genotypes (see Fig. S3). These results demonstrate that dysregulation of components of the E-C machinery is a secondary and progressive process in murine myotubular myopathy.

Impaired SR Calcium Release in Muscle Fibers from *Mtm1* KO Mice. These observations led us to investigate the functional properties of E-C coupling in muscle fibers from 5-week-old mice. For these measurements, short muscle fibers that are easily amenable to voltage-clamp, were isolated from the flexor digitorum brevis (FDB) and interosseus muscles. In these muscles, we also obtained evidence for partial loss of T-tubules in mutant fibers using confocal imaging of di-8-anneps fluorescence (*SI Methods* and Fig. S4).

Figure 3*A* shows indo-1 calcium signals recorded from a representative control and *Mtm1* mutant fiber, respectively. Ca^{2+} transients were triggered by voltage-clamp depolarizations of 5, 10, and 20 ms duration from −80 to +10 mV. The peak amplitude of the indo-1 transients was much smaller in the *Mtm1*-deficient fiber than in the control one, while the resting indo-1 level and the overall time-course of the transients were similar in the two fibers. Mean results from the indo-1 measurements on 14 fibers each revealed that the peak change in cytosolic calcium concentration ($\Delta[Ca^{2+}]$) was strongly depressed for all pulse durations in *Mtm1*-deficient fibers as compared to the values in control fibers ($P \leq 0.001$) (Fig. 3*B*). Conversely resting $[Ca^{2+}]$ levels were unaffected (Fig. 3*C*). The overall calcium removal capability of the cytosol including SR Ca^{2+} uptake was estimated from the rate of $[Ca^{2+}]$ decay after the end of the pulses. Exponential fits to the $[Ca^{2+}]$ decay time course showed that the rate was significantly depressed (by ≈30%, $P < 0.001$) following 5-ms-long pulses in mutant muscle cells, but this was not the case after longer pulses (Fig. 3*D*). This lower rate at 5-ms-long pulses may result from the very low peak $[Ca^{2+}]$ levels (< 0.5 μM) reached in response to this pulse in KO

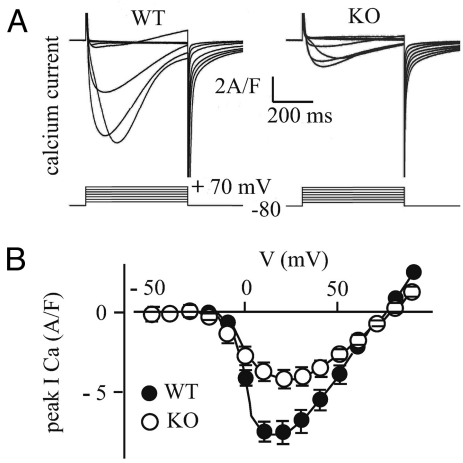

Fig. 4. Altered calcium channel function of the DHPR in 5-week-old mutant mice. (*A*) Ca^{2+} current records measured in response to 0.5-s-long depolarizing pulses to −50, −30, −10, +10, +30, +50, and + 70 mV in a WT (left) and myotubularin-deficient (right) muscle fiber. (*B*) Mean peak Ca^{2+} current versus voltage relationship of 16 muscle fibers from two WT mice and 20 fibers from two KO mice, under the conditions illustrated in panel *A*.

fibers, considering the strong [Ca^{2+}] dependence of the SR Ca^{2+} ATPase activity. To know whether the depressed peak Δ[Ca^{2+}] in the *Mtm1*-deficient fibers resulted from a decreased SR calcium content, we determined the total amount of releasable calcium by measuring indo-1 signals in fibers equilibrated with a large concentration of intracellular EGTA and challenged by a series of voltage-clamp depolarizations applied in the presence of a SR Ca^{2+} pump inhibitor. Results showed that the mean SR Ca^{2+} content did not significantly differ between control and *Mtm1*-deficient fibers (*SI Methods* and Fig. S4).

We next tested whether the depressed Ca^{2+} release in *Mtm1*-deficient fibers was related to an alteration of the properties of the voltage-sensor of E-C coupling, the DHPR. The voltage-activated Ca^{2+} current through the DHPR was measured in WT and *Mtm1*-deficient fibers. Figure 4*A* shows representative calcium current traces from a WT and from an *Mtm1*-deficient fiber in response to 0.5-s-long depolarizing pulses to various levels. The corresponding mean peak Ca^{2+} current density versus voltage relationships from identical measurements performed in 16 WT and 20 KO fibers are shown in Fig. 4*B*. Surprisingly, the peak amplitude of the Ca^{2+} current was strongly reduced in the *Mtm1*-deficient fibers. Fitting the individual current-voltage curves by a Boltzmann function scaled by the driving force (24) showed that this reduction corresponded to a 37% depression in the mean value for the maximal conductance of the calcium channels ($P < 0.03$). Overall results demonstrate that myotubularin deficiency is responsible for a severe functional alteration of both DHPR-mediated Ca^{2+} entry and RyR1-mediated SR Ca^{2+} release.

Discussion

In the present study, we show that absence of myotubularin in skeletal muscle induces alterations in the architecture of T-tubules and triads and a severe impairment of depolarization-induced Ca^{2+} release from the SR that is expected to lead to a reduced Ca^{2+}-troponin occupancy and thus to depressed contraction and force development.

The XLMTM mouse model used here reproduces major features of the corresponding human disease, including muscle weakness and hypotrophy, presence of internal nuclei in myofibers and fatal outcome within a few weeks after birth. The clinical and pathological evolution of the myopathy is more homogenous and also more severe in the 129PAS background than in the previously characterized C57/Bl6 XLMTM mice (20). We found that muscles are already affected in mice at 2 weeks of age as they contain hypotrophic fibers with altered distribution of triads, mitochondria, and, to some extent, nuclei. However, weakness was not yet apparent at this age. Importantly, as morphological abnormalities precede weakness, it suggests that defects noted at 2 weeks represent a primary event in disease pathogenesis.

Strikingly, we found an abnormal proportion of longitudinally oriented T-tubules and a reduced number of T-tubules/triads in *Mtm1*-deficient skeletal muscle, a phenomenon that increased over time. Abnormal oblique and longitudinal T-tubules have also been observed in muscle biopsies from some XLMTM patients (25). Longitudinal tubules are normally present in developing muscle before being rearranged, and this transition to a full transverse orientation occurs between birth and 3 weeks postnatally in mice (26). The presence of increased numbers of L-tubules and reduction of triads in 2-week-old *Mtm1*-deficient muscle suggests that the final rearrangement of this membranous system during early postnatal life does not occur properly in the absence of myotubularin. Although the molecular function of myotubularin in skeletal muscle is not well understood, additional findings support a role of myotubularin in T-tubule/SR network morphogenesis and/or remodeling. We previously showed that overexpression of myotubularin in myofibers alters plasma membrane homeostasis, leading to the accumulation of membrane saccules and vacuoles positive for sarcolemma markers (18). Moreover, amphiphysin 2, encoded by the *BIN1* gene is mutated in autosomal recessive cases of CNM, and its *Drosophila* ortholog is involved in the structural organization of the membrane compartment of the E-C coupling machinery (15, 27). The similar defects found both in our *Mtm1* KO mouse and in amphiphysin *Drosophila* mutants strongly support the existence of a common myotubularin-amphiphysin pathway regulating T-tubule biogenesis in muscle. Preliminary results indicate that the localization of amphiphysin 2 at the triad is partially decreased (manuscript in preparation). Caveolin 3 was also implicated in T-tubule biogenesis and is mutated in different forms of muscle diseases including limb-girdle muscular dystrophy type 1C (LGMD1C) (28, 29), highlighting the importance of this structure for human muscle function. Finally, while preparing this manuscript, a paper has described abnormalities in T-tubule organization in muscles from a zebrafish model of myotubular myopathy and patients (30).

Our analysis uncovered quantitative anomalies at mRNA and protein level in expression of genes related to the control of intracellular Ca^{2+} homeostasis. In skeletal muscle, myoplasmic Ca^{2+} concentration is tightly regulated, and its alteration severely affects muscle function (31, 32). The most striking change in myotubularin-deficient muscles was a drastic drop in the protein level of RyR1 Ca^{2+} release channel. Along this line, we found that Ca^{2+} release from the SR was strongly depressed in myotubularin-deficient fibers. Notably, the role of RyR1 in the pathogenesis of CNM is further supported by the recent finding of a de novo mutation in the *RYR1* gene in a patient with an autosomal dominant form (33). In contrast, we found that myoplasmic Ca^{2+} removal processes remained largely unaffected in *Mtm1*-deficient fibers, as demonstrated from our measurements of the rate of Ca^{2+} removal, SR Ca^{2+} content, and expression level of SERCA1. Our results also revealed that the SR Ca^{2+} release dysfunction in *Mtm1*-deficient fibers was associated with a decrease in the calcium channel activity of the DHPR, which is likely due to the decrease in DHPRα_1 protein level at the T-tubule membrane. In addition, the drop of RyR1 Ca^{2+} release channel protein may also contribute to this effect, because RyR1 per se was previously shown to be responsible for a retrograde coupling mechanism that specifically enhances the

function of DHPR as a voltage-dependent calcium channel (34). The decrease in DHPRα_1 protein level in *Mtm1* KO fibers may result from the drop in RyR1 level. Accordingly, skeletal muscle from mice lacking RyR1 was shown to exhibit a 2-fold reduction in the number of dihydropyridine binding sites. We also found an increase of DHPRβ_1 and γ_1 subunits mRNA. When examined at the protein level, DHPRβ_1 subunit was up-regulated by 6-fold in 5-week-old mutants. The β_1 subunit appears essential for the assembly of DHPR in arrays of tetrads at the junctional membrane (35), binds to RYR1, and strengthens E-C coupling (36). It is likely that the increased DHPRβ_1 level in *Mtm1* KO muscle results from a compensatory mechanism intended to promote targeting of newly expressed α_1 subunits to the triad and facilitate E-C coupling.

Taken together, our data favor a role of myotubularin in the physical organization of the E-C coupling machinery, at the T-tubules, and/or SR. However, we cannot exclude that it may also act directly on RyR1 channel function and/or protein transport and stability. For instance, mice deficient for mitsugumin-29 display similar ultrastructural abnormalities, but only minor defects in muscle strength (37). Myotubularin activity on PI(3)P and/or PI(3,5)P_2 could also play a direct role on channel activation, as previously reported for a homologous protein, MTMR6, which regulates the activity of the Ca^{2+}-activated K^+ channel KCa3.1 via PI(3)P (38, 39). Other mutant mice with deletions in genes involved in triad formation and/or calcium homeostasis, such as junctophilin 1 and triadin, also contain muscles with abnormally oriented T-tubules and alterations in Ca^{2+} transients and/or E-C coupling (40) (41). In conclusion, we propose that alterations in the structure of triads and defects in calcium homeostasis are the main cause of muscle weakness in centronuclear/myotubular myopathy. Manipulation of intracellular calcium in patient muscles may represent a therapeutic strategy.

Methods

Skeletal Muscle T-Tubule Labeling. WT and *Mtm1* KO mice in the 129PAS background were used in this study. Care and manipulation of mice were performed in accordance with national and European legislations on animal experimentation.

Immunohistochemistry. Anesthetized mice [by i.p. injection of 5 μL per body gram of ketamine (20 mg/mL; Virbac) and xylazine (0.4%, Rompun; Bayer)] were perfused with 4% paraformaldehyde before muscle dissection. Semithin sections (500-nm) of muscle were prepared as previously described (18). We used monoclonal antibodies directed against DHPRα_1 ($Ca_v1.1$) subunit (MA3–920; Affinity Bioreagents), RyR (clone 34C; Sigma), and SERCA1 ATPase (MA3–911; ABR).

Electron Microscopy. Selective staining of T-tubules in TA muscle was modified from (26). Briefly, muscles were dissected from anesthetized mice and fixed in 2.5% paraformaldehyde, 2.5% glutaraldehyde, and 50 mM $CaCl_2$ in 0.1 M cacodylate buffer (pH 7.4). Samples were postfixed with 2% OsO_4, 0.8% $K_3Fe(CN)_6$ in 0.1 M cacodylate buffer (pH 7.4) for 2 h at 4 °C and incubated with 5% uranyl acetate for 2 h at 4 °C. Muscles were dehydrated in a graded series of ethanol and embedded in epon resin. Thin (70-nm) sections were stained with uranyl acetate and lead citrate and examined by transmission electron microscope. The length of longitudinally oriented T-tubules and number of triads per Z-line were quantified with Metamorph 3 software from electron micrographs (magnification 9,800× and 5,600× for muscles of 5- and 2-week-old mice, respectively).

Quantitative RT-PCR Analysis. Total RNA was purified from muscles of 2- and 5-week-old male mice using TRIzol reagent (Invitrogen) according to manufacturer's instructions. cDNA was synthetized from 2–5 μg total RNA using SuperScript II reverse transcriptase (Invitrogen) and random hexamers. Quantitative PCR amplifications of cDNA were performed on Light-Cycler 480 and Light-Cycler 24 instruments (Roche) using 58 °C as melting temperature. Primer sequences for amplification are provided as *SI Methods*.

Immunoblot Analysis

Microsome Preparations. Frozen muscles were homogenized in 200 mM sucrose, 20 mM HEPES, 0.4 mM $CaCl_2$, pH 7.4, and protease inhibitors (1 mM PMSF, 100 μg/mL leupeptine) using a dounce tissue grinder (Wheaton). The supernatant obtained by centrifugation at 1,500 × *g* for 10 min, was further centrifuged at 41,000 × *g* for 50 min, and microsomes were resuspended in 0.1 M NaCl, 30 mM imidazole, 8% sucrose, pH 6.8, with protease inhibitors. All preparation steps are performed at 4 °C. Proteins were quantified with the Bio-Rad Laboratories Protein Assay detection kit and transferred to nitrocellulose membranes after electrophoresis in either 8 or 10% SDS polyacrylamide gels. Bands were scanned from photographic films by the Chemi Genius2 imaging system, and quantification was performed using GeneTools software (SynGene). The amount of protein was normalized against GAPDH as loading control.

Antibodies. Purified rabbit polyclonal antibody against mouse myotubularin was generated as previously described (18). We also used monoclonal antibodies directed against RyR1 (clone 34C; Sigma), DHPRβ subunit ($VD2_1$ B12; Developmental Studies Hybridoma Bank), SERCA1 ATPase (MA3–911; Affinity Bioreagents), calsequestrin (MA3–913; Affinity Bioreagents), glyceraldehyde-3-phosphate dehydrogenase (MAB374; Chemicon). Secondary horseradish peroxidase-conjugated antibodies against mouse and rabbit IgG (Jackson ImmunoResearch Laboratories) were detected using the ECL chemiluminescent reaction (Pierce).

Electrophysiology and Intracellular Calcium Measurements. Experiments were performed on single skeletal fibers from the FDB and interosseus muscles using previously described methods and analytical procedures (42–44), see *SI Methods* for further details.

Statistical Analysis. Data were statically analyzed using paired Student *t*-test. Values were considered significant when $P \leq 0.05$. Growth curves of mice were analyzed by ANOVA.

ACKNOWLEDGMENTS. We thank Yannick Schwab, Josiane Hergueux, and Yasmine Yucel for help in histological studies; all members of Institut de Génétique et de Biologie Moléculaire et Cellulaire (IGBMC) mouse house facility for help in animal care; and the Developmental Studies Hybridoma Bank, University of Iowa, Iowa City, IA, for providing $VD2_1$ B12 ascite. This study was supported by funds from the Institut National de la Santé et de la Recherche Médicale, the Centre National de la Recherche Scientifique, the Hôpital Universitaire de Strasbourg (HUS), the Collège de France and by grants from the Association Française contre les Myopathies (AFM), the Agence Nationale de la Recherche (ANR) and the Fondation pour la Recherche Médicale (FRM), the National Institutes of Health (P50 NS040828), the Joshua Frase Foundation, and the Lee and Penny Anderson Family Foundation. L.A.-Q. was supported by fellowships from the Syrian Ministry of High Education and the FRM.

1. Wallgren-Pettersson C, et al. (1995) The myotubular myopathies: Differential diagnosis of the X linked recessive, autosomal dominant, and autosomal recessive forms and present state of DNA studies. *J Med Genet* 32:673–679.
2. Pierson C, Tomczak K, Agrawal P, Moghadaszadeh B, Beggs AH (2005) X-linked myotubular and centronuclear myopathies. *J Neuropathol Exp Neurol* 64:555–564.
3. Jungbluth H, Wallgren-Pettersson C, Laporte J (2008) Centronuclear (myotubular) myopathy. *Orphanet J Rare Dis* 3:26.
4. Laporte J, et al. (1996) A gene mutated in X-linked myotubular myopathy defines a new putative tyrosine phosphatase family conserved in yeast. *Nat Genet* 13:175–182.
5. Laporte J, et al. (2000) MTM1 mutations in X-linked myotubular myopathy. *Hum Mutat* 15:393–409.
6. Biancalana V, et al. (2003) Characterisation of mutations in 77 patients with X-linked myotubular myopathy, including a family with a very mild phenotype. *Hum Genet* 112:135–142.
7. Blondeau F, et al. (2000) Myotubularin, a phosphatase deficient in myotubular myopathy, acts on phosphatidylinositol 3-kinase and phosphatidylinositol 3-phosphate pathway. *Hum Mol Genet* 9:2223–2229.
8. Taylor G, Maehama T, Dixon J (2000) Inaugural article: Myotubularin, a protein tyrosine phosphatase mutated in myotubular myopathy, dephosphorylates the lipid second messenger, phosphatidylinositol 3-phosphate. *Proc Natl Acad Sci USA* 97:8910–8915.
9. Tronchère H, et al. (2004) Production of phosphatidylinositol 5-phosphate by the phosphoinositide 3-phosphatase myotubularin in mammalian cells. *J Biol Chem* 278:7304–7312.
10. Cao C, Backer J, Laporte J, Bedrick E, Wandinger-Ness A (2008) Sequential actions of myotubularin lipid phosphatases regulate endosomal PI(3)P and growth factor receptor trafficking. *Mol Biol Cell* 19:3334–3346.
11. DiPaolo G, DeCamilli P (2006) Phosphoinositides in cell regulation and membrane dynamics. *Nature* 443:651–657.
12. Robinson F, Dixon J (2006) Myotubularin phosphatases: Policing 3-phosphoinositides. *Trends Cell Biol* 16:403–412.
13. Nicot A, Laporte J (2008) Endosomal phosphoinositides and human diseases. *Traffic* 9:1240–1249.
14. Bitoun M, et al. (2005) Mutations in dynamin 2 cause dominant centronuclear myopathy. *Nat Genet* 37:1207–1209.

15. Nicot A, et al. (2007) Mutations in amphiphysin 2 (BIN1) disrupt interaction with dynamin 2 and cause autosomal recessive centronuclear myopathy. *Nat Genet* 39:1134–1139.
16. Butler M, et al. (1997) Amphiphysin II (SH3P9; BIN1), a member of the amphiphysin/Rvs family, is concentrated in the cortical cytomatrix of axon initial segments and nodes of ranvier in brain and around T tubules in skeletal muscle. *J Cell Biol* 137:1355–1367.
17. Lee E, et al. (2002) Amphiphysin 2 (Bin1) and T-tubule biogenesis in muscle. *Science* 297:1193–1196.
18. Buj-Bello A, et al. (2008) AAV-mediated intramuscular delivery of myotubularin corrects the myotubular myopathy phenotype in targeted murine muscle and suggests a function in plasma membrane homeostasis. *Hum Mol Genet* 17:2132–2143.
19. Karpati G, Hilton-Jones D, Griggs R (2001) *Disorders of Voluntary Muscle* (Cambridge University Press, Cambridge, UK).
20. Buj-Bello A, et al. (2002) The lipid phosphatase myotubularin is essential for skeletal muscle maintenance but not for myogenesis in mice. *Proc Natl Acad Sci USA* 99:15060–15065.
21. Bevilacqua J, et al. (2009) ''Necklace'' fibers, a new histological marker of late-onset MTM1-related centronuclear myopathy. *Acta Neuropathol* 117:283–291.
22. Treves S, Jungbluth H, Muntoni F, Zorzato F (2008) Congenital muscle disorders with cores: The ryanodine receptor calcium channel paradigm. *Curr Opin Pharmacol* 8:319–326.
23. Beard N, Laver D, Dulhunty A (2004) Calsequestrin and the calcium release channel of skeletal and cardiac muscle. *Prog Biophys Mol Biol* 85:33–69.
24. Collet C, Csernoch L, Jacquemond V (2003) Intramembrane charge movement and L-type calcium current in skeletal muscle fibers isolated from control and mdx mice. *Biophys J* 84:251–265.
25. Sarnat H (1990) Myotubular myopathy: Arrest of morphogenesis of myofibres associated with persistence of fetal vimentin and desmin. Four cases compared with fetal and neonatal muscle. *Can J Neurol Sci* 17:109–123.
26. Franzini-Armstrong C (1991) Simultaneous maturation of transverse tubules and sarcoplasmic reticulum during muscle differentiation in the mouse. *Dev Biol* 146:353–363.
27. Razzaq A, et al. (2001) Amphiphysin is necessary for organization of the excitation-contraction coupling machinery of muscles, but not for synaptic vesicle endocytosis in *Drosophila*. *Genes Dev* 15:2967–2979.
28. Parton R, Way M, Zorzi N, Stang E (1997) Caveolin-3 associates with developing T-tubules during muscle differentiation. *J Cell Biol* 136:137–154.
29. Minetti C, et al. (1998) Mutations in the caveolin-3 gene cause autosomal dominant limb-girdle muscular dystrophy. *Nat Genet* 18:365–368.
30. Dowling J, et al. (2009) Loss of myotubularin function results in T-tubule disorganization in zebrafish and human myotubular myopathy. *PLoS Genet* 5:e1000372.
31. Gissel H (2005) The role of Ca^{2+} in muscle cell damage. *Ann N Y Acad Sci* 1066:166–180.
32. Dulhunty A (2006) Excitation-contraction coupling from the 1950s into the new millennium. *Clin Exp Pharmacol Physiol* 33:763–772.
33. Jungbluth H, et al. (2007) Centronuclear myopathy due to a de novo dominant mutation in the skeletal muscle ryanodine receptor (RYR1) gene. *Neuromuscul Disord* 17:338–345.
34. Nakai J, et al. (1996) Enhanced dihydropyridine receptor channel activity in the presence of ryanodine receptor. *Nature* 380:72–75.
35. Schredelseker J, et al. (2005) The beta 1a subunit is essential for the assembly of dihydropyridine-receptor arrays in skeletal muscle. *Proc Natl Acad Sci USA* 102:17219–17224.
36. Cheng W, Altafaj X, Ronjat M, Coronado R (2005) Interaction between the dihydropyridine receptor Ca^{2+} channel beta-subunit and ryanodine receptor type 1 strengthens excitation-contraction coupling. *Proc Natl Acad Sci USA* 102:19225–19230.
37. Nishi M, et al. (1999) Abnormal features in skeletal muscle from mice lacking mitsugumin29. *J Cell Biol* 147:1473–1480.
38. Srivastava S, et al. (2005) The phosphatidylinositol 3-phosphate phosphatase myotubularin- related protein 6 (MTMR6) is a negative regulator of the Ca^{2+}-activated K^{+} channel KCa3.1. *Mol Cell Biol* 25:3630–3638.
39. Srivastava S, et al. (2006) Phosphatidylinositol 3-phosphate indirectly activates KCa3.1 via 14 amino acids in the carboxy terminus of KCa3.1. *Mol Biol Cell* 17:146–154.
40. Ito K, et al. (2001) Deficiency of triad junction and contraction in mutant skeletal muscle lacking junctophilin type 1. *J Cell Biol* 154:1059–1067.
41. Shen X, et al. (2007) Triadins modulate intracellular Ca(2+) homeostasis but are not essential for excitation-contraction coupling in skeletal muscle. *J Biol Chem* 282:37864–37874.
42. Jacquemond V (1997) Indo-1 fluorescence signals elicited by membrane depolarization in enzymatically isolated mouse skeletal muscle fibers. *Biophys J* 73:920–928.
43. Collet C, Allard B, Tourneur Y, Jacquemond V (1999) Intracellular calcium signals measured with indo-1 in isolated skeletal muscle fibres from control and mdx mice. *J Physiol* 520:417–429.
44. Pouvreau S, Jacquemond V (2005) Nitric oxide synthase inhibition affects SR Ca^{2+} release in skeletal muscle fibres from mouse. *J Physiol* 567:815–823.